Rothamsted Repository Download

A - Papers appearing in refereed journals

De Souza, W. R., Martins, P. K., Freeman, J., Pellny, T. K., Michaelson, L. V., Sampaio, B. L., Vinecky, F., Ribeiro, A. P., Da Cunha, B. A. D. B., Kobayashi, A. K., De Oliveira, P. A., Campanha, R. B., Pacheco, T. F., Martarello, D. C. I., Marchiosi, R., Ferrarese-Filho, O., Dos Santos, W. D., Tramontina, R., Squina, F. M., Centeno, D. C., Gaspar, M., Braga, M. R., Tine, M. A. S., Ralph, J., Mitchell, R. A. C. and Molinari, H. B. C. 2018. Suppression of a single BAHD gene in Setaria viridis causes large, stable decreases in cell wall feruloylation and increases biomass digestibility. *New Phytologist.* 218 (1), pp. 81-93.

The publisher's version can be accessed at:

- https://dx.doi.org/10.1111/nph.14970

The output can be accessed at: https://repository.rothamsted.ac.uk/item/8450w.

1 **Suppression of a single BAHD gene in *Setaria viridis* causes large, stable**

2 **decreases in cell wall feruloylation and increases biomass digestibility**

3 Wagner R. de Souza[1†], Polyana K. Martins[1†], Jackie Freeman[2], Till K. Pellny[2],
4 Louise V. Michaelson[2], Bruno L. Sampaio[1], Felipe Vinecky[1], Ana P. Ribeiro[1],
5 Barbara A. D. B. da Cunha[1], Adilson K. Kobayashi[1], Patricia A. de Oliveira[1], Raquel
6 B. Campanha[1], Thályta F. Pacheco[1], Danielly C.I. Martarello[3], Rogério Marchiosi[3],
7 Osvaldo Ferrarese-Filho[3], Wanderley D. dos Santos[3], Robson Tramontina[4] , Fabio
8 M. Squina[5], Danilo d. Centeno[6], Marília Gaspar[7], Marcia R. Braga[7], Marco A. S.
9 Tiné[7], John Ralph[8], Rowan A. C. Mitchell[2]*, Hugo B. C. Molinari[1]*

10 [1] Embrapa Agroenergy, Brasília, DF, Brazil 70770901

11 [2]Plant Sciences, Rothamsted Research, Harpenden, Hertfordshire, AL5 2JQ, UK

12 [3] Department of Biochemistry, State University of Maringá, Maringá, Paraná, Brazil
13 87020-900

14 [4] Brazilian Bioethanol Science and Technology Laboratory, Brazilian Center for
15 Research in Energy and Materials, Campinas, Sao Paulo, Brazil 13083-100

16 [5] Programa de Processos Tecnológicos e Ambientais, Universidade de Sorocaba
17 (UNISO), Sorocaba, Brazil 18060-000

18 [6] Centre of Natural Sciences and Humanities, Federal University of ABC, São
19 Bernardo do Campo, SP, Brazil 09606-045

20 [7] Department of Plant Physiology and Biochemistry, Institute of Botany, Sao Paulo
21 04301-012, Brazil 04301-902

22 [8]Department of Biochemistry, and Department of Energy's Great Lakes Bioenergy
23 Research Center, Wisconsin Energy Institute, University of Wisconsin, Madison,
24 Wisconsin 537, USA

25 [†]These authors contributed equally to this work.

26 *Correspondence: RACM +44 1582 938469; rowan.mitchell@rothamsted.ac.uk.
27 HBCM +55 61 3448-2307; hugo.molinari@embrapa.br

28

29 Brief heading: "Suppression of a gene in grass species causes large decreases in
30 cell wall feruloylation" @Rothamsted

31

32 0 tables, 6 color figures. SI: 5 SI tables, 3 SI figures, 1 SI dataset.

33 Main text: 5,208 words. Summary 195 words.

SUMMARY

- Feruloylation of arabinoxylan (AX) in grass cell walls is a key determinant of recalcitrance to enzyme attack making it a target for improvement of grass crops, and of interest in grass evolution. Definitive evidence on the genes responsible is lacking so we studied a candidate gene that we identified within the BAHD acyl-CoA transferase family.

- We used RNAi silencing of orthologs in the model grasses *Setaria viridis* (*SvBAHD01*) and *Brachypodium distachyon* (*BdBAHD01*) and determined effects on AX feruloylation.

- Silencing of *SvBAHD01* in Setaria resulted in ~60% decrease in AX feruloylation in stems consistently across four generations. Silencing of *BdBAHD01* in Brachypodium stems decreased feruloylation by much smaller magnitude, possibly due to higher expression of functionally-redundant genes. Setaria *SvBAHD01* RNAi plants showed: no decrease in total lignin, ~doubled arabinose acylated by *p*-coumarate, changes in 2D-NMR spectra of unfractionated cell walls consistent with biochemical estimates, no effect on total biomass production, and an increase in biomass saccharification efficiency of 40-60%.

- We provide the first strong evidence for the key role of the *BAHD01* gene in AX feruloylation and demonstrate that it is a promising target for improvement of grass crops for biofuel, biorefining, and animal nutrition applications.

Keywords

cell wall acylation; ferulic acid; grass evolution; hydroxycinnamates; lignocellulosic feedstock

INTRODUCTION

Billions of tonnes of biomass, composed principally of secondary cell walls, are produced worldwide by grass crops annually either as the primary product for animal feed or as residues from food crops. Digestibility of this biomass – the ease with which sugar can be released from the cell wall polysaccharides – is a key economic target, both for the production of liquid biofuel and for efficiency of digestion by ruminant animals. A major distinguishing feature of grass cell walls and those of other commelinid monocots is the prevalence of two hydroxycinnamates, *p*-coumarate (*p*CA) and ferulate (FA) (Harris & Trethewey, 2010). FA, in particular is heavily involved in grass cell wall cross-linking reactions. The FA acylates arabinofuranosyl units that are 1→3-linked to the xylan backbone in arabinoxylan (AX) or glucuronoarabinoxylan (GAX). Ester-linked FA oxidatively couples in a similar manner to that of lignin monomers (Ralph *et al.*, 1992; Ralph *et al.*, 1995), forming cross-links with other (G)AX chains or with lignin (Ishii, 1997; Ralph *et al.*, 1998; Ralph *et al.*, 2004; Ralph, 2010). These cross-links inhibit digestion by preventing enzyme access and by tightly binding the polysaccharide substrate to non-digestible lignin. Decreasing FA content and thereby FA-mediated cross-linking of grass biomass has therefore long been considered a promising target in order to increase digestibility (de Oliveira *et al.*, 2015) and this is supported by: (a) *in vitro* studies showing inhibition by FA of polysaccharide saccharification to sugars (Grabber *et al.*, 1998a; Grabber *et al.*, 1998b); (b) natural variation in FA content being inversely correlated with digestibility (Lam *et al.*, 2003; Casler & Jung, 2006) (c) increasing biomass digestibility by heterologous expression of feruloyl esterase (Buanafina *et al.*, 2008); and (d) screens for increased digestibility in mutant populations that frequently identify low ferulate lines, e.g., (Hirano *et al.*, 2017).

Candidate genes involved in feruloylation of AX were first identified by differential expression between grasses and dicots (Mitchell *et al.*, 2007) as within a Clade of genes in the BAHD acyl-CoA transferase superfamily (there named "PF02458 family" after the characteristic PFAM domain). The most likely candidate within this clade for involvement in AX feruloylation based on absolute expression level and coexpression was identified as the rice gene LOC_Os01g09010 which we call here OsBAHD01. There are orthologs for this gene in all sequenced commelinid monocots; in *Brachypodium distachyon* (Brachypodium), *Setaria viridis* (Setaria) and

95   maize there is a one-to-one ortholog (see Figure 1A). Suppression of OsBAHD01 by

96   RNAi in rice was correlated with decreased cell wall FA (Piston *et al.*, 2010);

97   however, the FA decrease was variable between tissues and generations (largest

98   decrease was 27% in stems of one line) and the construct was designed to suppress

99   four other closely related genes as well as BAHD01. There is now strong evidence

100   that one of these (AT10) is specifically responsible for the acylation of AX by *p*-

101   coumarate (*p*CA) rather than FA (Bartley *et al.*, 2013). *p*CA is a hydroxycinnamate,

102   like FA, but crucially does not readily oxidatively couple *in vivo* and therefore does

103   not participate extensively in cross-links, although it may facilitate lignin

104   polymerization (Ralph, 2010). Others genes in the clade may also be responsible for

105   AX feruloylation; RNAi-suppression and overexpression of BdBAHD05 [Fig. 1A;

106   BdAT1 in the nomenclature from (Bartley *et al.*, 2013)] induced respective decreases

107   and increases in FA in transgenic Brachypodium lines (Buanafina *et al.*, 2016),

108   although the effects were relatively small (lines with biggest effects showed ~25%

109   decrease for RNAi, ~15% increase for overexpression). Effects on cell wall FA or

110   *p*CA due to manipulation of gene expression could be indirect, e.g., due to

111   perturbation of metabolite levels; this interpretation is made more plausible for the

112   (Piston *et al.*, 2010) and (Buanafina *et al.*, 2016) studies by the modest size of

113   effects on FA. Alternatively, they may be directly responsible for AX feruloylation but

114   compensatory mechanisms may operate or there may be gene redundancy within

115   the clade. Several of the genes are now known to encode enzymes that acylate

116   monolignols rather than AX by FA or *p*CA (Withers *et al.*, 2012; Petrik *et al.*, 2014;

117   Karlen *et al.*, 2016; Sibout *et al.*, 2016), leaving BAHD05 as putatively functionally

118   redundant with BAHD01 and three others (BAHD02, BAHD03, BAHD04; Fig. 1A)

119   with no functional indications.

120   *Setaria viridis* is an emerging monocot plant model for molecular and genetic

121   studies. It is a short, fast-growing, C4 plant with its genome sequence fully available

122   (Bennetzen *et al.*, 2012), and is in the same sub-family *Panicoideae* as sorghum,

123   maize and sugarcane. In addition, *S. viridis* is amenable to genetic transformation

124   through *Agrobacterium tumefaciens* (Martins *et al.*, 2015). Brachypodium is a model

125   C3 grass species in the same BOP clade of *Poaceae* as rice, wheat and *Lolium*

126   (Vogel *et al.*, 2010).

127   Here we show the effects of suppressing SvBAHD01 and BdBAHD01 expression in
128   Setaria and Brachypodium, respectively. Although the effects on cell wall FA in
129   Brachypodium are of similar magnitude to those reported previously for effects of
130   BAHD suppression, those in Setaria are much larger and more consistent. We
131   investigate possible reasons for this by examining the RNA-seq in transgenics of
132   both species. We also characterize the effects on cell walls, growth, and digestibility
133   of biomass in the Setaria transgenics and discuss the likely role of BAHD01 genes.

134

135

136 **MATERIAL AND METHODS**

137 **Phylogenetic analysis**

138 We downloaded protein sequences from Phytozome 12 (Goodstein *et al.*, 2012) for

139 the rice and Brachypodium BAHD candidate sequences identified (Mitchell *et al.*,

140 2007; Molinari *et al.*, 2013) and their orthologs in maize and Setaria. BdBAHD04

141 gene model is incorrect in Brachypodium v3 as shown by strand-specific RNA-seq

142 so we replaced with the v1 model. We performed alignment then optimization of

143 topology, parameters and branch length followed by bootstrapping as previously

144 described (Pellny *et al.*, 2012) but using PhyML3.0 (Guindon *et al.*, 2010). To identify

145 orthologs in 1KP database of plant transcriptomes (Wickett *et al.*, 2014), we

146 identified all hits with $E<10^{-5}$ using nucleotide blast (blastn) (Matasci *et al.*, 2014) with

147 rice candidate genes as queries; these were downloaded and assigned as ortholog

148 of top rice hit if bit score>100 using translated nucleotide searches against rice

149 proteome with Tera-BLASTP on the DeCypher® platform.

150

151 **Plasmid construct and Generation of Transgenic Plants**

152 For silencing of BAHD01 in both Setaria and Brachypodium, we selected a 254 bp

153 sequence with identical matches to both SvBAHD01 and BdBAHD01 (Figure S1A)

154 and no off-target identical matches of >16bp. Inverted repeats of this 254 bp flanking

155 the maize Adh2 intron were synthesised by Genscript, Piscataway, USA, and

156 subcloned into the transformation vector A224p6i-U-Gusi, using standard cloning

157 techniques, giving rise to the plasmid pITY73. In pITY73, the BAHD01 RNAi cassette

158 is under the control of the maize ubiquitin promoter. We transformed *Brachypodium*

159 inbred line Bd21 and *Setaria viridis* accession A10.1 following published protocols

160 (Vogel & Hill, 2008) and (24), respectively.

161

162 **RNA sequencing and differential expression analysis**

163 For Setaria, mRNA of stem from 3 replicate plants was obtained using NEBNext®

164 RNA Library Prep Set Kit for Illumina®. Libraries were made using NEB Next® Ultra

165 RNA Library Prep Kit and sequenced on an HiSeq4000 using TruSeq SBS v3 kit

166 (Illumina) by GenOne Biotechnologies. For Brachypodium, total RNA was isolated

167 from stems of minimum 3 replicate plants using protocol of (Chang *et al.*, 1993).

168 Libraries were made using the Ion Total RNA-Seq Kit v2, templates were prepared

169 using the Ion PITM Template OT2 200 Kit V2 and were sequenced using the Ion

170   PITM Sequencing 200 Kit v2 with an Ion PITM Chip Kit v2 on an Ion ProtonTM

171   System. All sequencing equipment and reagents were from Thermo Fisher Scientific

172   and used following the manufacturer's instructions. For both Setaria and

173   Brachypodium, reads were mapped to reference transcriptomes from Phytozome

174   11.0 using BWA-MEM algorithm (Li & Durbin, 2010) with default parameters for

175   Setaria and accepting forward reads only for the strand-specific reads generated by

176   Ion Proton sequencing for Brachypodium. Expression measures FPKM and CPM

177   were generated by the eXpress (Roberts & Pachter, 2013); global analysis to identify

178   all differentially expressed genes was performed using the edgeR package in R

179   (Robinson *et al.*, 2010). All reads and protocols have been deposited in public

180   database ArrayExpress accession E-MTAB-5648 for Setaria, E-MTAB-5649 for

181   Brachypodium.

182

183   **Quantification of cell-wall-bound hydroxycinnamate content**

184   Cell-wall-bound HCA content was determined essentially as described (Freeman *et*

185   *al.*, 2017) in labs at Embrapa Agroenergy (Table S1, Fig. S1C).and Rothamsted (Fig.

186   2, Table S2, Fig. S1D) and with some variations in protocol as described in SI

187   methods.

188

189   **Determination of HCA-conjugates released by mild acidolysis**

190   AIR was prepared using extractions as described for cell-wall-bound HCA and then

191   treated with 1.2 mL 50 mM trifluoroacetic acid for 4 h at 99 °C with agitation at 750

192   rpm. After centrifugation for 10 min at 16 000g 2 x 500 µL aliquots of supernatant

193   were freeze-dried. The pellet was washed twice with water and freeze-dried.

194   Released HCA-conjugates from one 500 µL aliquot of supernatant were dissolved in

195   250 µL 50% methanol:0.1% formic acid and 10 µL separated as for cell-wall-bound

196   HCA except using a binary gradient with methanol (solvent A) and 0.1% formic acid

197   (solvent B) with the following gradient: isocratic 100% B, 0-1 min; linear 100% to 0%

198   B, 1-21 min; isocratic 0% B, 21-23 min; linear 0% to 100% B, 23-28 min with a flow

199   rate of 1 mL/min. (We found this column provided much improved resolution over

200   that used in (Bartley *et al.*, 2013)). For mass spectrometry analysis samples were

201   diluted 1 in 8 and 10 µL was analysed on a 4000 QTRAP LC-MS/MS system

202   (SCIEX) after HPLC using an Agilent 1200 fitted with a 100-µL sample loop. The

203   probe was vertically positioned 11 mm from the orifice and charged with -4500 V.

204 Temperature was held at 750 °C, GS1 was set at 20 p.s.i., GS2 at 20 p.s.i., curtain

205 gas at 20 p.s.i., and the interface heater was engaged. MRM transitions were

206 derived from standards, previously published data (Quemener & Ralet, 2004; Bartley

207 *et al.*, 2013) and experimentally. Declustering potential, entrance potential, collision

208 energy and collision cell exit potential were set on an analyte-dependent basis

209 (Table S3). Data were collected with Analyst (SCIEX) software and integrated using

210 the Intelliquant algorithm. Peaks for individual analytes were assigned based on their

211 MRM transitions.

212

213 Quantitation of Ara-FA and Ara-*p*CA: Samples from mild acidolysis were run on a

214 Shimadzu Prominence HPLC with a photo-diode array detector using the same

215 column and protocol as for LC-MS. Area for peaks (absorbance at 280 nm) at

216 retention times corresponding to Ara-FA and Ara-*p*CA ions show the same relative

217 effects as ion counts across samples (Figure S2). Peak area relative to internal

218 standard peak area was used to quantify the peaks, using calibrations of

219 corresponding free HCA with pure standards. Values were multiplied by a correction

220 factor for difference in absorbance of Ara-HCA from free HCA, derived as follows.

221 Fractions for Ara-FA and Ara-*p*CA peaks were collected and split into two equal

222 samples, one of which was saponified, the other untreated. They were then re-run on

223 HPLC and correction factors calculated as (peak area free HCA) / (peak area Ara-

224 HCA) giving values of 0.92 and 0.62 for *p*CA and FA, respectively. This quantitation

225 of Ara-HCAs was conducted in Rothamsted lab to give data in Fig. 3. The same

226 procedure was used in Embrapa Agroenergy lab to give relative amounts in Fig. S3,

227 but using a Waters ACQUITY UPLC. To determine total ester-linked HCA following

228 mild acidolysis (Table S4), aliquots of supernatant and the pellet were saponified,

229 dried under vacuum, resuspended in 250 μL 50% methanol:0.1% formic acid, and

230 HCA content was quantified as in (Freeman *et al.*, 2017) but using the HPLC method

231 above used to separate HCA-conjugates.

232

233 **Cell wall characterization by solution-state 2D NMR**

234 We characterised the cell walls of Setaria samples without fractionation using

235 solution-state 2D NMR following procedure described by (Kim & Ralph, 2010); full

236 details are given in SI Methods.

237

Enzymatic saccharification assay

238

239   Samples of leaf and stem tissues of Ev.17.3, Ev.18.1 and NT at reproductive stage

240   were ground in a ball mill for 30 s and then subjected to enzymatic saccharification

241   with a commercially available enzyme preparation CellicCtec2 (Novozymes,

242   Denmark) at 10 FPU/g biomass. For biomass pre-treatment, 0.25% H_2SO_4 was

243   added and samples were incubated at 120 °C and 3.5 bar for 30 min. The enzymatic

244   hydrolysis (EH) experiments were performed using 2 mL Eppendorf tubes with 2%

245   (w/v) biomass in 100 mM phosphate buffer pH 5.0 and 0.1% sodium azide as an

246   antimicrobial agent. The reaction was incubated in a Thermomixer microplate

247   incubator (Eppendorf, Germany) operated at 50 °C and agitation speed of 1000 rpm.

248   Samples were withdrawn after 6 h, and the hydrolysis stopped by heating the

249   samples at 80 °C for 5 min, followed by centrifugation at 10,000 x g for 15 min. The

250   EH was measured by quantification of the glucose released according to the glucose

251   oxidase assay according to manufacturer's instructions.

252

Other Methods

253

254   Procedures based on published methods for determination of gene expression

255   (Martins *et al.*, 2016), cell wall monosaccharide (Sluiter *et al.*, 2012), lignin (Moreira-

256   Vilar *et al.*, 2014), growth conditions, biomass and stem microscopy are described in

257   detail in Methods S1.

258   **RESULTS**

259   **Identification of candidate BAHD gene for cell wall feruloylation and**
260   **generation of silencing lines in Setaria and Brachypodium**

261   We analyzed phylogeny of *BAHD* genes in the candidate clade [sometimes called
262   "Mitchell Clade"; (Bartley *et al.*, 2013)] for maize, *Brachypodium*, *Setaria*, rice and
263   Arabidopsis (Figure 1A). [Sub-clade B genes that show low expression, much less
264   conservation between species and no co-expression with cell wall genes (Molinari *et*
265   *al.*, 2013) are omitted]. Of the genes without direct functional evidence, BAHD01 is a
266   good candidate for cell wall feruloylation (Mitchell *et al.*, 2007; Bartley *et al.*, 2013;
267   Molinari *et al.*, 2013). Orthologs to OsBAHD01 are present in nearly all commelinid
268   monocots, but are almost completely absent from transcriptomes of other
269   angiosperms present in the 1KP database (Matasci *et al.*, 2014) (Fig. 1B), consistent
270   with the taxonomic distribution of (G)AX feruloylation (Harris & Trethewey, 2010). We
271   therefore selected Sevir.5G130000 (SvBAHD01) and its ortholog Bradi2g05480
272   (BdBAHD01) as targets for supression. We created a construct with an RNAi hairpin
273   designed to suppress both SvBAHD01 and BdBAHD01 under control of a
274   constitutive maize ubiquitin promoter (Figure S1A). We transformed Setaria with this
275   construct, obtaining 7 independent lines silencing SvBAHD01 61-99% in leaves that
276   showed decreases in FA of 39-60% (Table S1). We performed segregation analysis
277   through 2 generations (T_2 plants), obtaining 4 independent stable homozygous lines
278   compatible with single locus for Sv*BAHD01* RNAi transgene (Table S1). We
279   observed decreased contents of FA in the cell walls of leaf and stem tissues in these
280   transgenic lines (Figure S1C). We selected two of the best performing lines 17.3 and
281   18.1 for further detailed analysis. We also generated 6 independent homozygous
282   BdBAHD01 RNAi lines in Brachypodium; these showed only small effects on FA and
283   *p*CA (Table S2) and we selected two of these for further analysis.

284

285   **Cell wall hydroxycinnamate contents of SvBAHD01 RNAi Setaria plants and**
286   **BdBAHD01 Brachypodium RNAi plants**

287   To test the stability of *BAHD01* gene silencing and phenotype inheritance of altered
288   hydroxycinnamate composition in the cell walls of Setaria, we analyzed T_3

289   generation transgenic plants from the events 17.3 and 18.1. Silencing levels were

290   maintained in these plants; Sv*BAHD01* expression compared with non-transfromed

291   (NT) plants from the events 17.3 and 18.1 were 82% and 64% lower in leaves and

292   90% and 70% lower in stems, respectively (Fig. 2A). We observed a similar

293   reduction in FA contents in the cell walls of stem as seen in the T_0 and T_2

294   generations, corresponding to more than 60% decrease compared to NT plants, but

295   the decrease in FA in leaves was smaller than in T_2 (Fig. 2B). We found that ester-

296   linked *p*CA was more than doubled in the cell walls of leaves for the events 17.3 and

297   18.1 compared to control, whereas in the cell walls of stems we found only a small

298   increase (Fig. 2B). We also quantified the amounts of five different forms of

299   dehydrodiferulates (diFA); in leaves, the 8–8′-diFA coupled forms (8-8', 8-8' THF and

300   8-8' AT) were substantially decreased, with other diFAs unaffected (Fig. 2C). In

301   contrast, all diFAs except the aryltetralin form of 8–8′-diFA (8-8' AT) were decreased

302   in stems (Fig. 2C). Dimerisation expressed as sum of all diFA over total FA was

303   unaffected in leaves but highly significantly (P<0.001) increased in stems in both

304   lines (NT 25%, 17.3 37%, 18.1 35%). We found lignin content, as assessed by acetyl

305   bromide method, to be unchanged in stems of SvBAHD01 RNAi plants but with a

306   modest increase in leaves (Figure 2D).

307   We also analysed two Brachypodium BdBAHD01 RNAi lines for HCA content; these

308   also showed small (10–20%), but significant, decreases in FA and diFA content of

309   stem cell walls (Fig. S1E).

310   **Transcriptome analysis of transgenic SvBAHD01 and BdBAHD01 RNAi plants**

311   We analysed the RNA-seq transcriptomes from stems of T_3 SvBAHD01 and

312   BdBAHD01 RNAi plants in order to diagnose the difference in magnitude of the

313   effects of the transgenes in Setaria and Brachypodium, and also to test for off-target

314   and pleiotropic effects. We observed similar relative decreases in expression of

315   BdBAHD01 in Brachypodium line B5 (78%) as of SvBAHD01 in Setaria lines 17.3

316   and 18.1 (65%, 53%) (Figure 3). However, expression of SvBAHD01 was much

317   greater than BdBAHD01 in control lines, both in absolute FPKM values and,

318   importantly, relative to similar genes (Fig. 3), some of which may be functionally

319   redundant such as BAHD05 (Buanafina *et al.*, 2016). Greater relative expression of

320   redundant genes in Brachypodium could explain the much smaller effect of

321   BdBAHD01 suppression compared to SvBAHD01 suppression. We found no

322   evidence of a compensatory increase in expression of any BAHD genes in response

323   to BAHD01 suppression. SvBAHD09, an ortholog of BdPMT1, was significantly

324   down-regulated (Fig. 3); since there is little identity shared between SvBAHD09 and

325   the RNAi construct (longest identical sequence is 12bp), we interpret this as a

326   pleiotropic effect of suppressing SvBAHD01. Many other genes were also

327   significantly differentially regulated due to pleiotropic effects in both 17.3 and 18.1

328   (Notes S1), including upregulated genes associated with negative regulation of

329   transcription and protein synthesis and downregulated genes associated with

330   cytoskeleton and xylan synthesis and remodelling.

331   As the effects of BAHD01 suppression were much greater in Setaria than

332   Brachypodium, we focussed on characterising the SvBAHD01 RNAi lines in more

333   detail.

334

Characterization of xylan in SvBAHD01 RNAi plants

336   Bound FA and diFA are ester-linked to arabinofuranosyl units attached to

337   glucuronoarabinoxylan (GAX) of grass cell walls (Scheller & Ulvskov, 2010); we

338   found no consistent effect on Ara and Xyl content of AIR (predominantly derived from

339   GAX) in SvBAHD01 RNAi plants (Table S5). We analysed Ara-HCAs using mild

340   acidolysis with TFA of AIR which preferentially breaks glycosidic Ara-(1→3)-Xyl

341   linkages in GAX, but can break other linkages releasing GAX oligosaccharides and

342   free HCAs, and can chemically modify the Ara-HCA (Saulnier *et al.*, 1995; Bartley *et*

343   *al.*, 2013). We developed a novel method which identifies peaks from LC-MS for Ara-

344   FA, Ara-*p*CA and minor peaks with m/z of parent/daughter ions 649/589 and 457/193

345   (Table S3; Fig. 4A). These minor peaks are consistent with Ara-diFA-Ara and Xyl-

346   Ara-FA (Table S3), being derived respectively from a xylan-diFA-xylan cross-link and

347   from the 2-β-Xyl*p*-(5-feruloyl)-Ara*f* decoration of xylan that is common in grasses

348   (Wende & Fry, 1997).

349   Using peak areas in UV absorbance spectra from this method, we found ~30% and

350   ~70% decreases in Ara-FA caused by SvBAHD01 silencing in leaves and stems

351   respectively (Fig. 4B). This Ara-FA accounts for about 40% of the FA monomer in all

352   samples (Table S4), so relative effects are similar to those for FA (Fig. 2). (The

353   remainder of the FA monomer in TFA-treated samples is present in other forms;

354   Tables S4, S5). Ara-pCA was increased by SvBAHD01 silencing to about double in

355   both leaves and stems, although the absolute amount is low in stems (Fig. 4B).

356   To test the stability of the silencing, we repeated analyses of Ara-HCAs in T_4

357   generation plants (Figure S3). We observed essentially the same effect of

358   SvBAHD01 silencing on Ara-FA as in T_3; a ~65% decrease in stems and ~35%

359   decrease in leaves The increases in Ara-pCA were more variable, ranging from 30%

360   to 150% (Fig. S3).

361   Total ester-linked pCA from cell walls is comprised of Ara-pCA and lignin-pCA, with

362   lignin-pCA being much more abundant in stems than in leaves. Lignin-pCA is

363   enriched in the pellet fraction following mild acidolysis; we found increases in pCA in

364   this fraction in leaves of SvBAHD01 RNAi T_3 and T_4 plants (Table S4) to be of similar

365   magnitude to the Ara-pCA increases (Fig. 4; Fig. S3), but in stems the increases

366   were inconsistent and smaller. This suggests that lignin-pCA was increased similarly

367   to Ara-pCA in leaves but not stems of SvBAHD01 RNAi plants.

368

369

370   **2D-NMR characterization of cell walls in SvBAHD01 RNAi plants**

371   To gain information on the overall aromatic composition of the unfractionated cell

372   walls in the SvBAHD01 silenced plants, we analyzed them using gel-state 2D NMR

373   (Kim & Ralph, 2010). We observed clear differences in the spectral fingerprints

374   between control and SvBAHD01 RNAi plants in both leaves and stems, showing the

375   expected decrease in FA peaks (Fig. 5). The magnitude of the decrease as

376   estimated from the normalized integrals shown in Fig. 5 (~50%) is similar to that

377   estimated from biochemistry (~60%; Fig. 2) for stems but much greater in leaves

378   (~70% for 2D-NMR compared to ~10% in Fig. 2). The 2D-NMR values are on a lignin

379   basis and it is known that the integrals of small mobile components such as FA and

380   pCA relative to those for relatively immobile internal lignin units are significantly over-

381   represented and variable in this methodology. The changes in FA : pCA ratios show

382   better agreement between the 2D-NMR and biochemical methods, respectively -58%

383 and -65% in leaves, and -71% and -73% in stems. The smaller effect of SvBAHD01
384 silencing on this ratio in roots (-33%) compared to other tissues is also consistent
385 with the smaller effect we saw on FA content of roots using the biochemical assay
386 (Fig. S1C).

387

Plant biomass, seed yield, saccharification and stem microscopy in SvBAHD01
388
389 **RNAi plants**

390 We observed no significant changes in aerial biomass associated with the
391 SvBAHD01 RNAi plants (Fig. 6A), but there was a significant small (8%) decrease in
392 seed size (Fig. 6B) and an apparent increase in seed number in line 18.1(Fig. 6C).
393 We assessed ease of saccharification of biomass from transgenic plants pretreated
394 or not with H_2SO_4 0.25%. We found that levels of glucose released by transgenic
395 plants were significantly higher compared with NT plants, both for treated and non-
396 treated samples, in both tissues, indicating a more efficient saccharification of
397 SvBAHD01 RNAi plants' biomass (Fig. 6D). In cross-sections of stems, we observed
398 that the walls of sclerenchyma and parenchyma cells of SvBAHD01 RNAi plants
399 were less thick than those of control plants (Fig. 6E). We also observed a change in
400 staining with phloroglucinol in interfascicular sclerenchyma which were pale yellow in
401 SvBAHD01 RNAi plants in contrast to bright yellow of controls (Fig. 6E i-iii), possibly
402 related to presence of benzaldehydes (Akin, 1990). Both staining with auramine O
403 (Fig. 6E iv-vi) and autofluorescence (Fig. 6E vii-ix) of vascular bundle cells and
404 interfascicular sclerenchyma were somewhat decreased, consistent with decreased
405 cell wall phenolic content.

406

DISCUSSION

BAHD01 was identified as a candidate for involvement in the feruloylation of GAX ten years ago, along with other genes in the same clade (Mitchell *et al.*, 2007). There was some early evidence for this role for BAHD01 from RNAi suppression of several genes together (BAHD01, 02, 04, 08 and 10) in rice in which decreases of FA of 10-30% were observed (Piston *et al.*, 2010). However, this construct simultaneously suppressed expression of other genes including one since implicated in the addition of *p*CA, not FA, to GAX [BAHD10/ AT10; (Bartley *et al.*, 2013)] and an ortholog of BdPMT2 (BAHD08) putatively involved in addition of *p*CA to lignin (Sibout *et al.*, 2016). We are not aware of any reports of knock-out mutants for BAHD01, nor of *in vitro* activity assays for the encoded protein, both of which have been reported for the closely related lignin PMT genes (Withers *et al.*, 2012; Marita *et al.*, 2014; Petrik *et al.*, 2014). The characterization of this gene has therefore lagged behind that of PMT despite the importance of feruloylation in determining properties of grass biomass.

Moderate changes, that vary between generations (Piston *et al.*, 2010; Buanafina *et al.*, 2016) in cell wall FA due to suppression and overexpression of BAHD genes, can be interpreted as secondary effects; however, the large, consistent effects that we observed from suppressing SvBAHD01 on FA content in Setaria generations T_0, T_2,T_3,T_4 (Table S1; Fig. S1C; Fig. 2; Fig. 4; Fig. S3) make this interpretation less plausible. Our results on the effect on cell wall FA of suppressing BdBAHD01 in Brachypodium were more like these previous reports in magnitude (Fig. S1E). Our transcriptome analysis offers one possible explanation for the greater magnitude of the effect in Setaria than in Brachypodium; SvBAHD01 is more highly expressed compared to BdBAHD01 relative to other candidate BAHD genes (Fig. 3). In particular, BdBAHD05 may have the same function as BdBAHD01 as suppression and overexpression of this gene induced respective decreases and increases in FA (Buanafina *et al.*, 2016). Of total BAHD01 and BAHD05 transcript abundance in stems of control plants, SvBAHD01 accounts for 83% in Setaria whereas BdBAHD01 only accounts for 56% in Brachypodium. There is no evidence of a compensatory upregulation of other BAHD transcripts in response to BAHD01 suppression in either species (Fig. 3). The relative lack of effect of BdBAHD01 suppression may therefore be due to greater redundancy in Brachypodium, or simply that the suppression was

440 insufficient to limit feruloylation in this species; identification of BdBAHD01 knock-out
441 mutants would address this possibility.

442 Other genes within the phenylpropanoid pathway leading to monolignol biosynthesis
443 were not differentially expressed in SvBAHD01 RNAi stems (Notes S1) and total
444 lignin was unaffected in stems (Fig. 2D). We found evidence from 2D-NMR of
445 decreased **S/G** ratio in stems but not leaves (Fig. 5); estimates of **H** lignin units are
446 not reliable from this method due to overlapping protein signals (Kim *et al.*, 2017).
447 We assumed, as is common, that all FA and diFA released by mild alkali from AIR is
448 ester-linked to arabinofuranose on GAX. In fact, as monolignol ferulates are now
449 firmly established monomers in the lignification of monocots, such compounds could
450 in principle also result from this lignin source; however, as ferulates and diferulates
451 are well incorporated into lignins by radical coupling reactions, the extremely low
452 released levels of such components can be neglected here (Karlen *et al.*, 2016). This
453 assumption was supported by quantitation of Ara*f*-FA released by mild acidolysis
454 from SvBAHD01 RNAi lines (Fig. 4). We observed similar relative effects of
455 SvBAHD01 silencing as for total FA, decreases of 65-65% from stems and 30-35%
456 from leaves in T_3 (Fig. 4B) and T_4 (Fig. S3) generation plants. An unexpected result
457 was the increase in *p*CA observed in leaves, but not stems, of both SvBAHD01 RNAi
458 lines (Fig. 2B). There are two forms of ester-linked *p*CA in grass cell walls; those
459 acylating Ara*f* on GAX and those acylating the lignin sidechain (Ralph, 2010). Ara*f*-
460 *p*CA content more than doubled due to SvBAHD01 suppression in both leaves and
461 stems (Fig. 4B), but this only accounts for a proportion of the total *p*CA in leaves,
462 and a smaller proportion in stems. BAHD genes like OsAT10 (our BAHD10) are
463 likely responsible for the Ara*f*-*p*CA whereas the BAHD PMT genes are responsible
464 for the addition of *p*CA to monolignols, and hence its appearance on lignin, but none
465 of the BAHD genes showed significant upregulation in SvBAHD01 RNAi plants (Fig.
466 3). One possible explanation for the increased cell wall *p*CA is that the blocking of
467 addition of FA to Ara*f* results in a build-up of FA-CoA and *p*CA-CoA substrates; the
468 increased *p*CA-CoA concentration results in more *p*CA addition to GAX in both
469 stems and leaves. There also seems to be increased lignin-*p*CA in leaves of
470 SvBAHD01 RNAi plants; in stems, SvBAHD09 transcript, a putative PMT, was
471 downregulated (Fig. 3), which could be a regulatory response to prevent excessive
472 addition of *p*CA to lignin.

473

474   All BAHD proteins are believed to be localized to the cytosol and this has been

475   confirmed using a GFP fusion of TaBAHD01 for the wheat ortholog (J. Freeman,

476   unpublished), but feruloylation of GAX takes place within the Golgi (Myton & Fry,

477   1994; Fry, 2004). It has therefore been suggested (Buanafina, 2009) that a cytosolic

478   precursor such as UDP-Ara*f* is the acceptor for FA or *p*CA, as their CoA thioesters,

479   mediated by these BAHD enzymes; as UDP-Ara*f* is generated in the cytosol by

480   UDP-arabinopyranose mutase, this is feasible. The feruloylated UDP-Ara*f* would

481   then pass into the Golgi by a transporter (possibly encoded by grass homologs of the

482   recently identified UDP-Ara*f* transporters in Arabidopsis (Rautengarten *et al.*, 2017))

483   and FA-Ara*f* would be transferred onto GAX, most likely by GT61 enzymes that are

484   responsible for arabinosylation of xylan (Anders *et al.*, 2012). In support of this

485   model, RNAi Brachypodium lines with decreased mutase (Rancour *et al.*, 2015) and

486   the rice *xax1* mutant which carries a knockout for a GT61 family gene (Chiniquy *et*

487   *al.*, 2012) both showed substantial decreases in cell wall FA; in contrast to our

488   results for SvBAHD01 suppression, they also both showed decreased cell wall *p*CA.

489   This may suggest that specificity for FA or *p*CA is conferred exclusively by the BAHD

490   enzymes in this pathway.

491   Biomass production was unaffected by SvBAHD01 suppression (Fig. 6A) and ease

492   of saccharification was increased (Fig. 6D). However, there were some pleiotropic

493   effects; the many differentially regulated transcripts in the SvBAHD01 RNAi lines

494   suggest shifts in development, protein synthesis and increased stress responses

495   (Notes S1) and there was significantly decreased seed size (Fig. 6B) and changes in

496   stem morphology (Fig. 6E). Ferulate mediated cross-linking is fundamental to both

497   primary and secondary cell walls in grasses and it is not surprising that constitutive

498   suppression has downstream consequences; directing the suppression to secondary

499   cell walls specifically (as achieved elsewhere (Yang *et al.*, 2013)) might decrease

500   pleiotropic effects whilst maintaining benefit in digestibility. The large increase in

501   biomass saccharification that we observed in SvBAHD01 RNAi plants (Fig. 6D)

502   indicates that BAHD01 represents a promising target to increase the suitability of

503   grass biomass for biofuel and animal feed applications. The effect appears relatively

504   specific to affecting FA linked to GAX but not total lignin (Fig. 2D), compared with

505   modification of genes responsible for earlier steps in the phenylpropanoid pathway

506 (e.g., (Bouvier d'Yvoire *et al.*, 2013)). We would predict that it results in fewer
507 covalent linkages between the polysaccharide and lignin components of cell walls
508 (as well as between polysaccharides themselves), allowing greater ease of
509 separation, e.g., for biorefining, but this remains to be demonstrated. Indeed, it has
510 been demonstrated that, in a model system, the rate and extent of wall hydrolysis by
511 fungal enzymes is affected by ferulate-mediated polysaccharide cross-linking
512 (Grabber *et al.*, 1998a) and even more by lignin-polysaccharide cross-linking, as
513 reviewed (Ralph *et al.*, 1998; Ralph, 2010). Greater understanding of the role of
514 BAHD01 and related genes will help identify opportunities for grass crop
515 improvement and elucidate the importance of cell wall feruloylation in grass
516 evolution.

517

518

519

530

AUTHOR CONTRIBUTIONS

H.B.C.M, J.F., R.A.C.M, and T.K.P. planned and designed research. W.R.d.S., P.K.M., J.F., T.K.P., L.V.M., B.L.S., F.V., A.P.R., B.A.D.B.d.C., A.K.K., P.A.d.O., R. B., T.F.P., D.C.I.M., R.M., O.F., W.D.d.S., R.T., F.M.S, D.d.C., M.G., M.R., M.A.S.T., J.R., R.A.C.M., H.B.C.M. performed research and/or analyzed data. R.A.C.M. wrote the manuscript with contributions from H.B.C.M., J.R., P.K.M. and W.R.d.S.

537

538

19

REFERENCES

Akin DE. 1990. Diazonium compounds localize grass cell wall phenolics: relation to wall digestibility. *Crop Science* **v. 30**(no. 5): pp. 985-989-1990 v.1930 no.1995.

Anders N, Wilkinson MD, Lovegrove A, Freeman J, Tryfona T, Pellny TK, Weimar T, Mortimer JC, Stott K, Baker JM, et al. 2012. Glycosyl transferases in family 61 mediate arabinofuranosyl transfer onto xylan in grasses. *Proceedings of the National Academy of Sciences of the United States of America* **109**(3): 989-993.

Bartley LE, Peck ML, Kim SR, Ebert B, Manisseri C, Chiniquy DM, Sykes R, Gao LF, Rautengarten C, Vega-Sanchez ME, et al. 2013. Overexpression of a BAHD acyltransferase, *OsAt10*, alters rice cell wall hydroxycinnamic acid content and saccharification. *Plant Physiology* **161**(4): 1615-1633.

Bennetzen JL, Schmutz J, Wang H, Percifield R, Hawkins J, Pontaroli AC, Estep M, Feng L, Vaughn JN, Grimwood J, et al. 2012. Reference genome sequence of the model plant Setaria. *Nat Biotechnol* **30**(6): 555-561.

Bouvier d'Yvoire M, Bouchabke-Coussa O, Voorend W, Antelme S, Cézard L, Legée F, Lebris P, Legay S, Whitehead C, McQueen-Mason SJ, et al. 2013. Disrupting the cinnamyl alcohol dehydrogenase 1 gene (BdCAD1) leads to altered lignification and improved saccharification in Brachypodium distachyon. *The Plant Journal* **73**(3): 496-508.

Buanafina MMD, Fescemyer HW, Sharma M, Shearer EA. 2016. Functional testing of a PF02458 homologue of putative rice arabinoxylan feruloyl transferase genes in Brachypodium distachyon. *Planta* **243**(3): 659-674.

Buanafina MMDO, Langdon T, Hauck B, Dalton S, Morris P. 2008. Expression of a fungal ferulic acid esterase increases cell wall digestibility of tall fescue (Festuca arundinacea). *Plant Biotechnology Journal* **6**(3): 264-280.

Buanafina MMO. 2009. Feruloylation in grasses: current and future perspectives. *Mol Plant* **2**(5): 861-872.

Casler MD, Jung HJG. 2006. Relationships of fibre, lignin, and phenolics to in vitro fibre digestibility in three perennial grasses. *Animal Feed Science and Technology* **125**(1-2): 151-161.

Chang S, Puryear J, Cairney J. 1993. A simple and effecient method for isolating RNA from pine trees. *Plant Molecular Biology Reporter* **11**: 113-116.

Chiniquy D, Sharma V, Schultink A, Baidoo EE, Rautengarten C, Cheng K, Carroll A, Ulvskov P, Harholt J, Keasling JD, et al. 2012. XAX1 from glycosyltransferase family 61 mediates xylosyltransfer to rice xylan. *Proceedings of the National Academy of Sciences of the United States of America* **109**(42): 17117-17122.

Considine JA, Knox RB. 1979. Development and histochemistry of the cells, cell walls, and cuticle of the dermal system of fruit of the grape,Vitis vinifera L. *Protoplasma* **99**(4): 347-365.

de Oliveira DM, Finger-Teixeira A, Mota TR, Salvador VH, Moreira-Vilar FC, Molinari HBC, Mitchell RAC, Marchiosi R, Ferrarese O, dos Santos WD. 2015. Ferulic acid: a key component in grass lignocellulose recalcitrance to hydrolysis. *Plant Biotechnology Journal* **13**(9): 1224-1232.

Freeman J, Ward JL, Kosik O, Lovegrove A, Wilkinson MD, Shewry PR, Mitchell RAC. 2017. Feruloylation and structure of arabinoxylan in wheat endosperm cell walls from RNAi lines with suppression of genes responsible for backbone synthesis and decoration. *Plant Biotechnol J* **15**(11): 1429–1438.

Fry SC. 2004. Primary cell wall metabolism: tracking the careers of wall polymers in living plant cells. *New Phytologist* **161**(3): 641-675.

Goodstein DM, Shu SQ, Howson R, Neupane R, Hayes RD, Fazo J, Mitros T, Dirks W, Hellsten U, Putnam N, et al. 2012. Phytozome: a comparative platform for green plant genomics. *Nucleic Acids Research* **40**(D1): D1178-D1186.

588   **Grabber JH, Hatfield RD, Ralph J. 1998a.** Diferulate cross-links impede the enzymatic degradation of
589   non-lignified maize walls. *Journal of the Science of Food and Agriculture* **77**(2): 193-200.
590   **Grabber JH, Ralph J, Hatfield RD. 1998b.** Severe inhibition of maize wall degradation by synthetic
591   lignins formed with coniferaldehyde. *Journal of the Science of Food and Agriculture* **78**(1):
592   81-87.
593   **Guindon S, Dufayard JF, Lefort V, Anisimova M, Hordijk W, Gascuel O. 2010.** New algorithms and
594   methods to estimate maximum-likelihood phylogenies: assessing the performance of PhyML
595   3.0. *Systematic Biology* **59**(3): 307-321.
596   **Harris PJ, Trethewey JAK. 2010.** The distribution of ester-linked ferulic acid in the cell walls of
597   angiosperms. *Phytochemistry Reviews* **9**(1): 19-33.
598   **Hirano K, Masuda R, Takase W, Morinaka Y, Kawamura M, Takeuchi Y, Takagi H, Yaegashi H,
599   Natsume S, Terauchi R, et al. 2017.** Screening of rice mutants with improved saccharification
600   efficiency results in the identification of CONSTITUTIVE PHOTOMORPHOGENIC 1 and GOLD
601   HULL AND INTERNODE 1. *Planta* **246**(1): 61-74.
602   **Ishii T. 1997.** Structure and functions of feruloylated polysaccharides. *Plant Science* **127**(2): 111-127.
603   **Karlen SD, Peck ML, Zhang C, Smith RA, Padmakshan D, Helmich KE, Free HCA, Lee S, Smith BG, Lu
604   F, et al. 2016.** Monolignol ferulate conjugates are naturally incorporated into plant lignins.
605   *Science Advances* **2**(10): 1-9.
606   **Kim H, Ralph J. 2010.** Solution-state 2D NMR of ball-milled plant cell wall gels in DMSO-d_6/pyridine-
607   d_5. *Organic & Biomolecular Chemistry* **8**(3): 576-591.
608   **Kim H, Padmakshan D, Li Y, Rencoret J, Hatfield RD, Ralph J. 2017.** Characterization and elimination
609   of undesirable protein residues in plant cell wall materials for enhancing lignin analysis by
610   solution-state NMR. *Biomacromolecules*: in press (10.1021/acs.biomac.7b01223).
611   **Lam TBT, Iiyama K, Stone BA. 2003.** Hot alkali-labile linkages in the walls of the forage grass Phalaris
612   aquatica and Lolium perenne and their relation to in vitro wall digestibility. *Phytochemistry*
613   **64**(2): 603-607.
614   **Li H, Durbin R. 2010.** Fast and accurate long-read alignment with Burrows-Wheeler transform.
615   *Bioinformatics* **26**(5): 589-595.
616   **Marita JM, Hatfield RD, Rancour DM, Frost KE. 2014.** Identification and suppression of the p-
617   coumaroyl CoA:hydroxycinnamyl alcohol transferase in Zea mays L. *The Plant Journal* **78**(5):
618   850-864.
619   **Martins PK, Mafra V, de Souza WR, Ribeiro AP, Vinecky F, Basso MF, da Cunha BADB, Kobayashi
620   AK, Molinari HBC. 2016.** Selection of reliable reference genes for RT-qPCR analysis during
621   developmental stages and abiotic stress in Setaria viridis. *Scientific Reports* **6**: 28348
622   **Martins PK, Ribeiro AP, Cunha BADBd, Kobayashi AK, Molinari HBC. 2015.** A simple and highly
623   efficient Agrobacterium-mediated transformation protocol for Setaria viridis. *Biotechnology*
624   *Reports* **6**: 41-44.
625   **Matasci N, Hung LH, Yan ZX, Carpenter EJ, Wickett NJ, Mirarab S, Nguyen N, Warnow T,
626   Ayyampalayam S, Barker M, et al. 2014.** Data access for the 1,000 Plants (1KP) project.
627   *Gigascience* **3**: 17.
628   **Mitchell RAC, Dupree P, Shewry PR. 2007.** A novel bioinformatics approach identifies candidate
629   genes for the synthesis and feruloylation of arabinoxylan. *Plant Physiology* **144**(1): 43-53.
630   **Molinari HB, Pellny TK, Freeman J, Shewry PR, Mitchell RA. 2013.** Grass cell wall feruloylation:
631   distribution of bound ferulate and candidate gene expression in *Brachypodium distachyon*.
632   *Frontiers in Plant Science* **4**: 50.
633   **Moreira-Vilar FC, Siqueira-Soares Rde C, Finger-Teixeira A, de Oliveira DM, Ferro AP, da Rocha GJ,
634   Ferrarese Mde L, dos Santos WD, Ferrarese-Filho O. 2014.** The acetyl bromide method is
635   faster, simpler and presents best recovery of lignin in different herbaceous tissues than
636   Klason and thioglycolic acid methods. *PLoS ONE* **9**(10): e110000.
637   **Myton KE, Fry SC. 1994.** Intraprotoplasmic feruloylation of arabinoxylans in *Festuca arundinacea* cell
638   cultures. *Planta* **193**(3): 326-330.

639   **Pellny TK, Lovegrove A, Freeman J, Tosi P, Love CG, Knox JP, Shewry PR, Mitchell RAC. 2012.** Cell
640   walls of developing wheat starchy endosperm: comparison of composition and RNA-seq
641   transcriptome. *Plant Physiology* **158**(2): 612-627.
642   **Petrik DL, Karlen SD, Cass CL, Padmakshan D, Lu FC, Liu S, Le Bris P, Antelme S, Santoro N,**
643   **Wilkerson CG, et al. 2014.** *p*-Coumaroyl-CoA:monolignol transferase (PMT) acts specifically
644   in the lignin biosynthetic pathway in *Brachypodium distachyon*. *Plant Journal* **77**(5): 713-726.
645   **Piston F, Uauy C, Fu LH, Langston J, Labavitch J, Dubcovsky J. 2010.** Down-regulation of four
646   putative arabinoxylan feruloyl transferase genes from family PF02458 reduces ester-linked
647   ferulate content in rice cell walls. *Planta* **231**(3): 677-691.
648   **Quemener B, Ralet MC. 2004.** Evidence for linkage position determination in known feruloylated
649   mono- and disaccharides using electrospray ion trap mass spectrometry. *Journal of Mass*
650   *Spectrometry* **39**(10): 1153-1160.
651   **Ralph J. 2010.** Hydroxycinnamates in lignification. *Phytochemistry Reviews* **9**(1): 65-83.
652   **Ralph J, Bunzel M, Marita JM, Hatfield RD, Lu F, Kim H, Schatz PF, Grabber JH, Steinhart H. 2004.**
653   Peroxidase-dependent cross-linking reactions of *p*-hydroxycinnamates in plant cell walls.
654   *Phytochemistry Reviews* **3**: 79-96.
655   **Ralph J, Grabber JH, Hatfield RD. 1995.** Lignin-ferulate cross-links in grasses: active incorporation of
656   ferulate polysaccharide esters into ryegrass lignins. *Carbohydrate Research* **275**(1): 167-178.
657   **Ralph J, Hatfield RD, Grabber JH, Jung HG, Quideau S, Helm RF 1998.** Cell wall cross-linking in
658   grasses by ferulates and diferulates. . In: Lewis NG, Sarkanen S eds. *Lignin and Lignan*
659   *Biosynthesis*. Washington, DC: American Chemical Society, 209-236.
660   **Ralph J, Helm RF, Quideau S, Hatfield RD. 1992.** Lignin feruloyl ester cross-cinks in grasses .1.
661   Incorporation of feruloyl esters into coniferyl alcohol dehydrogenation polymers. *Journal of*
662   *the Chemical Society-Perkin Transactions 1*(21): 2961-2969.
663   **Rancour DM, Hatfield RD, Marita JM, Rohr NA, Schmitz RJ. 2015.** Cell wall composition and
664   digestibility alterations in Brachypodium distachyon achieved through reduced expression of
665   the UDP-arabinopyranose mutase. *Front Plant Sci* **6**: 446.
666   **Rautengarten C, Birdseye D, Pattathil S, McFarlane HE, Saez-Aguayo S, Orellana A, Persson S, Hahn**
667   **MG, Scheller HV, Heazlewood JL, et al. 2017.** The elaborate route for UDP-arabinose
668   delivery into the Golgi of plants. *Proceedings of the National Academy of Sciences* **114**(16):
669   4261-4266.
670   **Roberts A, Pachter L. 2013.** Streaming fragment assignment for real-time analysis of sequencing
671   experiments. *Nat Meth* **10**(1): 71-73.
672   **Robinson MD, McCarthy DJ, Smyth GK. 2010.** edgeR: a Bioconductor package for differential
673   expression analysis of digital gene expression data. *Bioinformatics* **26**(1): 139-140.
674   **Saulnier L, Vigouroux J, Thibault JF. 1995.** Isolation and partial characterization of feruloylated
675   oligosaccharides from maize bran. *Carbohydrate Research* **272**(2): 241-253.
676   **Scheller HV, Ulvskov P. 2010.** Hemicelluloses. *Annual Review of Plant Biology* **61**: 263-289.
677   **Sibout R, Le Bris P, Legee F, Cezard L, Renault H, Lapierre C. 2016.** Structural redesigning
678   Arabidopsis lignins into alkali-soluble lignins through the expression of p-coumaroyl-coA:
679   monolignol transferase PMT. *Plant Physiology* **170**(3): 1358-1366.
680   **Sluiter A, Hames B, Ruiz R, Scarlata C, Sluiter J, Templeton D, Crocker D. 2012.** Determination of
681   Structural Carbohydrates and Lignin in Biomass. National laboratory of the U.S. Department
682   of Energy, Office of Energy Efficiency & Renewable Energy Technical Reports.
683   **Vogel J, Hill T. 2008.** High-efficiency *Agrobacterium*-mediated transformation of *Brachypodium*
684   *distachyon* inbred line Bd21-3. *Plant Cell Reports* **27**(3): 471-478.
685   **Vogel JP, Garvin DF, Mockler TC, Schmutz J, Rokhsar D, Bevan MW, Barry K, Lucas S, Harmon-Smith**
686   **M, Lail K, et al. 2010.** Genome sequencing and analysis of the model grass Brachypodium
687   distachyon. *Nature* **463**(7282): 763-768.
688   **Wende G, Fry SC. 1997.** 2-O-beta-D-xylopyranosyl-(5-O-feruloyl)-L-arabinose, a widespread
689   component of grass cell walls. *Phytochemistry* **44**(6): 1019-1030.

690 **Wickett NJ, Mirarab S, Nguyen N, Warnow T, Carpenter E, Matasci N, Ayyampalayam S, Barker MS,**
691   **Burleigh JG, Gitzendanner MA, et al. 2014.** Phylotranscriptomic analysis of the origin and
692   early diversification of land plants. *Proceedings of the National Academy of Sciences of the*
693   *United States of America* **111**(45): E4859-E4868.
694 **Withers S, Lu FC, Kim H, Zhu YM, Ralph J, Wilkerson CG. 2012.** Identification of grass-specific
695   enzyme that acylates monolignols with *p*-coumarate. *Journal of Biological Chemistry*
696   **287**(11): 8347-8355.
697 **Yang F, Mitra P, Zhang L, Prak L, Verhertbruggen Y, Kim J-S, Sun L, Zheng K, Tang K, Auer M, et al.**
698   **2013.** Engineering secondary cell wall deposition in plants. *Plant Biotechnology Journal*
699   **11**(3): 325-335.

700

701 **SUPPORTING INFORMATION LIST**

702 Methods S1. Procedures for plant growth, microscopy and determination of gene

703 expression, cell wall monosaccharide, lignin and biomass.

704 Table S1. SvBAHD01 silencing, FA content and segregation in Setaria SvBAHD01

705 RNAi lines.

706 Table S2. HCAs content of Brachypodium and Setaria samples.

707 Table S3. MRMs and identities of most prevalent ions released from AIR samples by

708 mild acidolysis.

709 Table S4. HCA content of saponified samples following mild acidolysis from Setaria

710 plants.

711 Table S5. Monosaccharide composition of cell walls from Setaria plants.

712 Figure S1. RNAi construct, and HCA content of Brachypodium and Setaria RNAi

713 plants.

714 Figure S2. LC-MS chromatograms and correlations of UV absorbance and MRM ion

715 count peak areas.

716 Figure S3. HCA-Ara content for T_4 Setaria samples.

717 Notes S1. Differentially expressed transcripts in SvBAHD01 RNAi stems from RNA-

718 seq.

719

720   **FIGURE LEGENDS**

721   Figure 1. A. Phylogenetic tree of candidate clade of BAHD genes (Mitchell *et al.*,

722   2007) showing BAHD names for each branch from (Molinari *et al.*, 2013) and

723   alternative AT names from (Bartley *et al.*, 2013). All genes from Arabidopsis, rice,

724   Brachypodium, maize and Setaria in sub-clade A are shown. Support for topology is

725   shown as percentage of bootstrap runs. Named genes have evidence on function

726   from [1] (Withers *et al.*, 2012) [2] (Bartley *et al.*, 2013) [3] (Petrik *et al.*, 2014) [4]

727   (Marita *et al.*, 2014) [5] (Buanafina *et al.*, 2016) [6] (Sibout *et al.*, 2016) [7] (Karlen *et*

728   *al.*, 2016). Asterisks mark the genes we studied here. B: Distribution of orthologs

729   present in 1KP project (Matasci *et al.*, 2014) to the candidate rice genes and to

730   related OsHCT genes. Proportions of species (out of total number shown at top of

731   grid) that have orthologs are shown as blue pie chart slices.

732

733   Figure 2. SvBAHD01 gene expression (A) and ester-linked HCA and lignin content

734   (B,C,D) of cell walls in leaves and stems of Setaria control (NT) and T_3 plants from

735   17.3 and 18.1 RNAi-silenced lines (n=3; error bars SEM; significance of difference of

736   transgenic from control indicated if difference in means > LSD from ANOVA at

737   *P<0.05, **P<0.01, ***P<0.001).

738   Figure 3. RNA-seq analysis of BAHD gene expression in Setaria SvBAHD01 RNAi

739   lines and Brachypodium BdBAHD01 RNAi lines. Genes associated with monolignol

740   acylation (PMT and FMT) are indicated. Transcript abundance measure is fragment

741   per kilobase per million mapped reads (FPKM; n=3; error bars SEM; significance of

742   difference of transgenic from control indicated if difference in means > LSD from

743   ANOVA at *P<0.05, **P<0.01, ***P<0.001).

744   Figure 4. HCA-conjugates in supernatant follwing mild acidolysis of Setaria AIR. (A)

745   Parts of representative HPLC chromatograms showing UV absorbtion. Major peaks

746   *p*CA-Ara and FA-Ara were identified by LC-MS (Supplemental Fig. S2; Table S3).

747   *p*CA co-elutes with an unknown UV-absorbing compound. Minor peaks are labelled

748   by their dominant parent/daugther ion m/z from LC-MS; 649/589 and 457/193 are

749   probably Ara-diFA-Ara and Xyl-Ara-FA, respectively. (B) Mean *p*CA-Ara and FA-Ara

750   contents expressed as μg HCA equivalent per mg AIR estimated from similar

751   chromatograms as shown in A (n=3; error bars SEM; significance of difference of

752   transgenic from control indicated if difference in means > LSD from ANOVA at
753   *P<0.05, **P<0.01, ***P<0.001).

754

755   Figure 5. 2D-NMR HSQC (heteronuclear single-quantum coherence) partial spectra
756   of stem, leaf, and root tissues from the WT control (NT) and the two transgenic lines
757   (17.3 and 18.1) of Setaria. Color coding of the contours matches that of the assigned
758   structures; where contour overlap occurs, the colorization is only approximate. The
759   analytical data are from volume-integrals of correlation peaks representing
760   reasonably well-resolved (except for **H**) C/H pairs in similar environments; thus they
761   are from $\mathbf{S}_{2/6}$, $\mathbf{G}_2$, $\mathbf{H}_{2/6}$, $\mathbf{FA}_2$, $\boldsymbol{pCA}_{2/6}$ and $\mathbf{T}_{2'/6'}$, with obvious correction for those units
762   that have two C/H pairs per unit. All relative integrals are on a G+S=100% basis; H-
763   units are over-quantified due to an overlapping peak from protein phenylalanine
764   (Phe) units (Kim *et al*., 2017).

765   Figure 6. Biomass (A), seed size (B) and number (C), saccharification (D) and stem
766   morphology (E) of Setaria *SvBAHD01* RNAi plants. A-D: Means and SEM from 10
767   (A, B) or 5 (C, D) replicate plants, significance of difference of transgenic from
768   control indicated if difference in means > LSD from ANOVA at *P<0.05, **P<0.01,
769   ***P<0.001. E: Representative stem sections from NT (i, iv, vii), 17.3 (ii, v, viii) and
770   18.1 plants (iii, vi, ix) stained with phloroglucinol (i - iii), auramine O (iv – vi) and
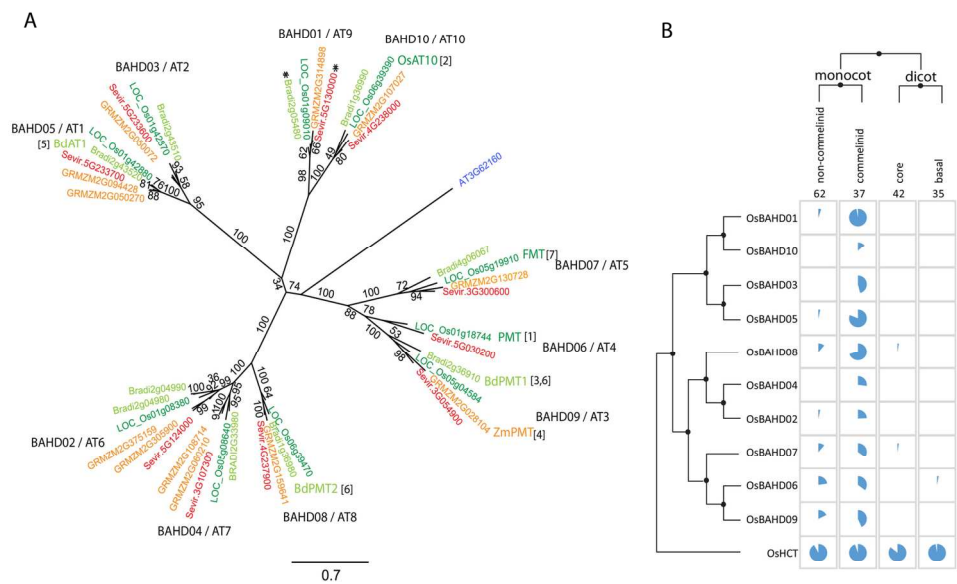771   showing autofluorsence (vii – ix).

772

773

Figure 1. A. Phylogenetic tree of candidate clade of BAHD genes (Mitchell et al., 2007) showing BAHD names for each branch from (Molinari et al., 2013) and alternative AT names from (Bartley et al., 2013). All genes from Arabidopsis, rice, Brachypodium, maize and Setaria in sub-clade A are shown. Support for topology is shown as percentage of bootstrap runs. Named genes have evidence on function from [1] (Withers et al., 2012) [2] (Bartley et al., 2013) [3] (Petrik et al., 2014) [4] (Marita et al., 2014) [5] (Buanafina et al., 2016) [6] (Sibout et al., 2016) [7] (Karlen et al., 2016). Asterisks mark the genes we studied here. B: Distribution of orthologs present in 1KP project (Matasci et al., 2014) to the candidate rice genes and to related OsHCT genes. Proportions of species (out of total number shown at top of grid) that have orthologs are shown as blue pie chart slices.

148x108mm (300 x 300 DPI)

Figure 2. SvBAHD01 gene expression (A) and ester-linked HCA and lignin content (B,C,D) of cell walls in leaves and stems of Setaria control (NT) and T3 plants from 17.3 and 18.1 RNAi-silenced lines (n=3; error bars SEM; significance of difference of transgenic from control indicated if difference in means > LSD from ANOVA at *P<0.05, **P<0.01, ***P<0.001).

230x176mm (300 x 300 DPI)

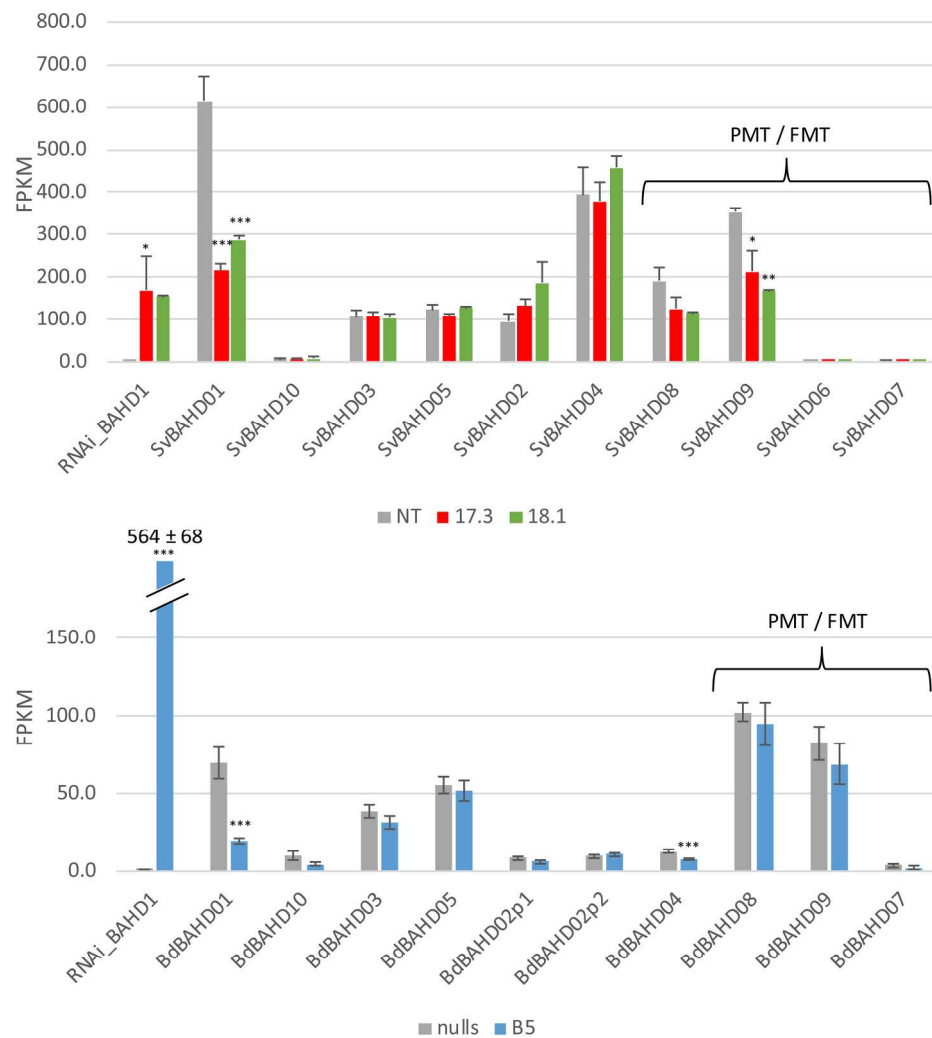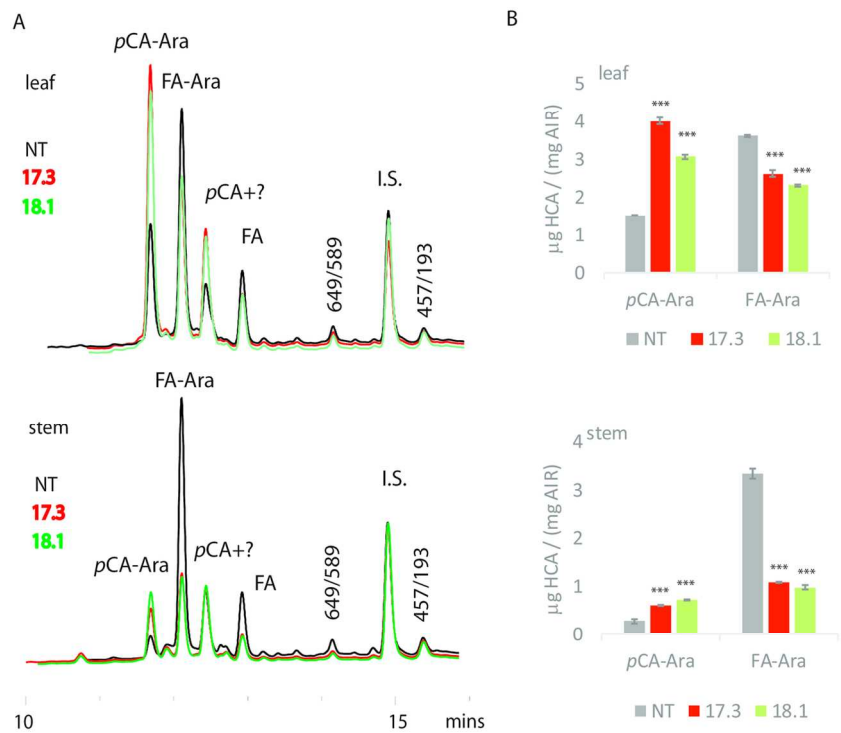Figure 3. RNA-seq analysis of BAHD gene expression in Setaria SvBAHD01 RNAi lines and Brachypodium BdBAHD01 RNAi lines. Genes associated with monolignol acylation (PMT and FMT) are indicated. Transcript abundance measure is fragment per kilobase per million mapped reads (FPKM; n=3; error bars SEM; significance of difference of transgenic from control indicated if difference in means > LSD from ANOVA at *P<0.05, **P<0.01, ***P<0.001).

203x217mm (300 x 300 DPI)

Figure 4. HCA-conjugates in supernatant follwing mild acidolysis of Setaria AIR. (A) Parts of representative HPLC chromatograms showing UV absorbtion. Major peaks pCA-Ara and FA-Ara were identified by LC-MS (Supplemental Fig. S2; Table S3). pCA co-elutes with an unknown UV-absorbing compound. Minor peaks are labelled by their dominant parent/daugther ion m/z from LC-MS; 649/589 and 457/193 are probably Ara-diFA-Ara and Xyl-Ara-FA, respectively. (B) Mean pCA-Ara and FA-Ara contents expressed as µg HCA equivalent per mg AIR estimated from similar chromatograms as shown in A (n=3; error bars SEM; significance of difference of transgenic from control indicated if difference in means > LSD from ANOVA at *P<0.05, **P<0.01, ***P<0.001).
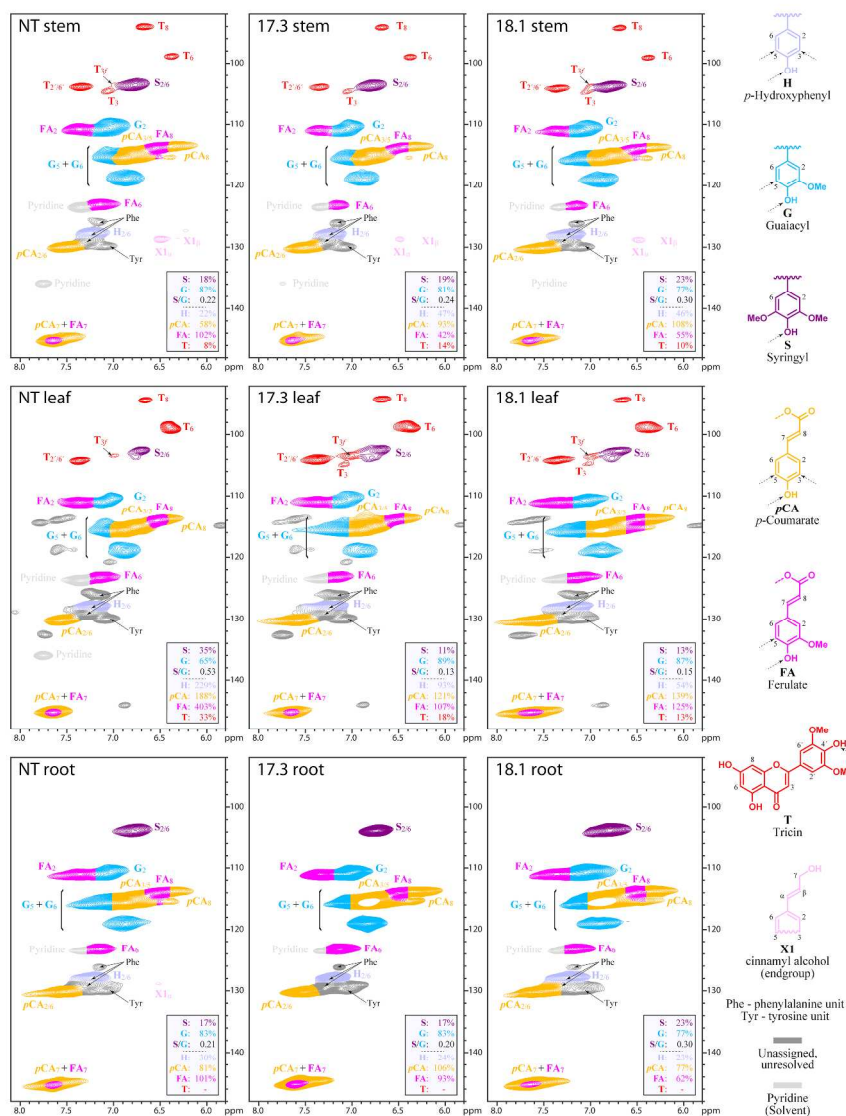
132x96mm (300 x 300 DPI)

Figure 5. 2D-NMR HSQC (heteronuclear single-quantum coherence) partial spectra of stem, leaf, and root tissues from the WT control (NT) and the two transgenic lines (17.3 and 18.1) of Setaria. Color coding of the contours matches that of the assigned structures; where contour overlap occurs, the colorization is only approximate. The analytical data are from volume-integrals of correlation peaks representing reasonably well-resolved (except for H) C/H pairs in similar environments; thus they are from S2/6, G2, H2/6, FA2, pCA2/6 and T2′/6′, with obvious correction for those units that have two C/H pairs per unit. All relative integrals are on a G+S=100% basis; H-units are over-quantified due to an overlapping peak from protein phenylalanine (Phe) units (Kim et al., 2017).
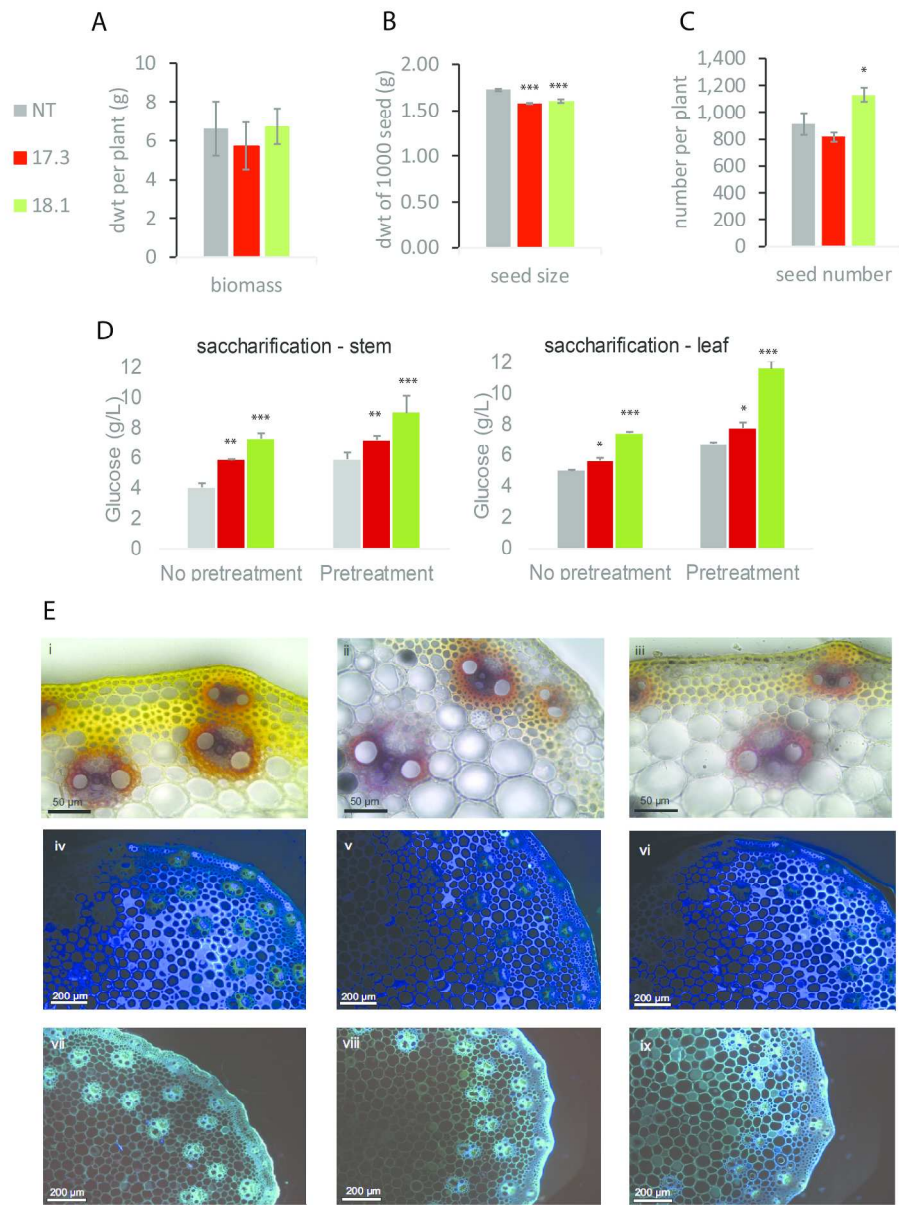
279x361mm (300 x 300 DPI)

Figure 6. Biomass (A), seed size (B) and number (C), saccharification (D) and stem morphology (E) of Setaria SvBAHD01 RNAi plants. A-D: Means and SEM from 10 (A, B) or 5 (C, D) replicate plants, significance of difference of transgenic from control indicated if difference in means > LSD from ANOVA at *P<0.05, **P<0.01, ***P<0.001. E: Representative stem sections from NT (i, iv, vii), 17.3 (ii, v, viii) and 18.1 plants (iii, vi, ix) stained with phloroglucinol (i - iii), auramine O (iv – vi) and showing autofluorsence (vii – ix).

219x285mm (300 x 300 DPI)